Desalination and Water Treatment
www.deswater.com

doi: 10.5004/dwt.2022.28766

271 (2022) 143–156
September

Adsorption performance and mechanism of lake sludge-derived ball milling biochar loaded with Fe_3O_4 on Cd(II) in aqueous solution

Dian Lv

School of Civil Engineering, Architecture and Environment, Hubei University of Technology, Wuhan 430068, China, email: 101900551@hbut.edu.cn

Received 30 March 2022; Accepted 23 July 2022

ABSTRACT

In this paper, air-dried lake sludge was pretreated by ball milling, and then pyrolysed at 600°C to prepare lake sludge-derived ball milling biochar, and Fe_3O_4 was loaded on lake sludge-derived ball milling biochar by chemical precipitation. Scanning electron microscopy-energy-dispersive X-ray spectroscopy, Fourier-transform infrared spectroscopy, and X-ray diffraction were used to investigate and characterize the adsorbents. The results demonstrated that ball mill pretreatment and Fe_3O_4-loaded can effectively increase the content of O-containing groups in the adsorbent. The batch adsorption experiments revealed that Cd(II) removal followed the pseudo-second-order kinetic model and the Langmuir model. Additionally, the Cd(II) maximum adsorption by biochar (BC), MBBC and Fe_3O_4@MBBC was 31.33, 47.36 and 92.42 mg/g, respectively. The Cd(II) removal mechanisms were complexation, ion exchange, co-precipitation and electrostatic interaction. The Cd(II) removal efficiency on Fe_3O_4@MBBC was maintained at 91.35% after 5 adsorption–desorption experiments, indicating that Fe_3O_4@MBBC had the ability to be better applied for the removal of Cd(II)-containing wastewater.

Keywords: Ball milling; Lake sludge-derived ball milling biochar; Fe_3O_4; Cd(II); Adsorption; Mechanism

1. Introduction

With the economic development in China, many heavy metals have entered the natural environment such as water bodies through various channels, posing a serious threat to the ecological environment and even human health [1–3]. Heavy metal Cd(II) pollution is a serious environmental problem in China [4]. Cd(II) easily migrates and is easily enriched into the human body through the food chain, and accumulates and destroys in the bones, liver and kidneys of the human body [5–7]. Because of this, there is a great need to investigate how to remove Cd(II) ions from aqueous solutions. Adsorption has been favoured by researchers in recent years as a simple, inexpensive and effective method [8].

Biochar, a black carbon-rich material produced by pyrolysis of biomass raw materials in an anoxic or anaerobic atmosphere, has a large specific surface area, well-developed pores, abundant functional groups and a stable structure [9–12]. Therefore, in recent years, many scholars have used various types of biochar for the removal of Cd(II) from aqueous solutions, such as eucalyptus leaf biochar [5], peanut shell biochar [10] and cow dung-derived vermicompost biochar [13]. To further enhance the heavy metals adsorption capacity of biochar, researchers have used a range of modification methods to treat the biochar, such as acid-base modification, inorganic mineral modification, metal oxide loading and microwave radiation [14–19]. However, these modification methods

are complex, chemically dependent and prone to produce hazardous waste. A simpler and greener process needs to be found for biochar modification. Ball milling technology is an emerging technology that has the advantages of being green, low cost, easy to operate and mass produced when applied to biochar modification [16,20–22]. Xiao et al. [23] find that the adsorption capacity of Cd(II), Cu(II) and Pb(II) by N-containing ball milling biochar prepared from bovine bone meal is 165.77, 287.58 and 558.88 mg/g, respectively, representing increases of 93.91%, 75.56% and 64.61% compared with the un-milled preparation. Cui et al. [16] find that the adsorption capacities of corn stover-derived biochar (BC), ball-milled corn stover-derived biochar (B-BC) and MgAl-LDHs-modified ball-milled corn stover-derived biochar (B-LDHs-BC) are 57.4, 72.1 and 105 mg/g for Cd(II), respectively. The above studies have shown that ball milling technology can effectively increase the heavy metals adsorption capacity of biochar. Ball milling can increase the specific surface area and improve the pore structure of biochar, thus providing more adsorption sites for the adsorption of heavy metals [20,22]. Besides, previous studies have demonstrated that the O-containing groups of the adsorbent can be increased by ball milling [21,22].

In this paper, lake sludge-derived ball milling biochar loaded with Fe_3O_4 (Fe_3O_4@MBBC) was prepared from Fe_3O_4 and lake sludge. The objectives were to (1) study the effect of ball mill pretreatment on the adsorption performance of biochar; (2) investigate the effects of reaction time, temperature, pH, coexisting ions, background ion and initial Cd(II) concentration on the Cd(II) removal, and (3) analyse the removal mechanism.

2. Materials and methods

2.1. Reagents

Fe_3O_4 pellets were purchased from Shanghai Aladdin Reagent Co., Ltd., (Shanghai, China). $Cd(NO_3)_2$, NaCl, NaOH and HCl were all analytically reagent (AR) and purchased from Sinopharm Chemical Reagent Co., Ltd., (Shanghai, China). The experiment water was deionized water (DW). Different mass concentrations of Cd storage solution were prepared by $Cd(NO_3)_2$.

2.2. Preparation of biochar and modified biochar

Preparation of lake sludge-derived ball milling biochar [24]: The lake sludge was taken from the bottom of a lake in Wuhan and firstly dried in a ventilated place for 7 d. The lake sludge was then dried to constant weight in a constant temperature drying oven (DF205, Hebei Haowei Electric Equipment Technology Co., Ltd., China) at 80°C. The dried lake sludge was subjected to ball milling in a ball mill (JC-QM, Qingdao Juchuang Environmental Protection Group Co., Ltd., China) and the sieved sludge powder was collected after passing through an 80 mesh sieve. The sludge powder was placed in a crucible and placed in a tube furnace with N_2 as protective gas, heated to 600°C at a rate of 20°C/min and pyrolysed for 2 h and then cooled. The powder was neutralized with deionized water, dried for storage, and recorded as MBBC. Besides, no ball milling pretreatment of the feedstock was carried out and the lake sludge-derived biochar was prepared by the above steps and recorded as BC.

Lake sludge-derived ball milling biochar loaded with Fe_3O_4 composite (Fe_3O_4@MBBC) [25]: BC with Fe_3O_4 in a mass ratio of 1:1 was added to 300 mL of DW, the solution pH was adjusted to 10.0~11.0 with NaOH (1 mol/L), and then stirred in a water bath at 90°C and 180 rpm for 12 h. After the stirring was completed, the mixture was centrifuged and the resulting solid was collected. The powder was washed with DW to neutral. The solid was then dried in a desiccator at 80°C for 12 h, after which it was written down as Fe_3O_4@MBBC.

2.3. Batch adsorption experiments

10 mg of absorbent and 25 mL of Cd(II) solution were mixed. The mixture solution pH was adjusted with 0.1 mol/L of HCl and NaOH, and then reacted in a constant temperature shaker at 150 rpm and 25°C for a certain time. The influence factors of initial pH (2.0~8.0), 10~50 mg/L of coexisting ions (Na^+, K^+, Ni^{2+}, Pb^{2+}, Cu^{2+}, Fe^{3+} and Al^{3+}), background ion (NaCl, 0~1 mol/L), adsorption time (5–480 min), temperature (15°C, 25°C and 35°C) and initial Cd(II) concentration (10~150 mg/L) of the solutions were investigated on the Cd(II) removal.

Simulation of the species distribution of Cd(II) in aqueous solution was carried out using the Visual MINTEQ 3.1. The conditions simulated were a temperature of 25°C and a Cd(II) concentration of 10 mg/L. The solutions that reached adsorption equilibrium were centrifuged and filtered, and the Cd(II) concentration in the filtrate was determined using flame atomic absorption spectrophotometry (AA-6300, Shimadzu, Japan), and the removal efficiency [Eq. (1)] and adsorption capacity [Eq. (2)] were calculated.

$$R = \frac{C_0 - C_e}{C_0} \times 100\% \tag{1}$$

$$Q = \frac{(C_0 - C_e) \times V}{m} \tag{2}$$

where R is the removal efficiency, %; C_0 is the initial Cd(II) mass concentration in solution, mg/L; C_e is the Cd(II) mass concentration in solution after adsorption equilibrium, mg/L; q_e is the equilibrium adsorption capacity, mg/g; V/m is the ratio of solution volume to adsorbent mass, mL/mg.

2.4. Adsorption–desorption experiments

At 25°C, pH 6.0 and Cd(II) concentration of 10 mg/L, 10 mg biochar was mixed with 25 mL Cd solution and reacted in a shaker for 480 min. After completion of the reaction, the solution was filtered and the adsorbed biochar was collected. The adsorbed biochar was added to 1 mol/L HCl and desorbed for 12 h in a shaker. After desorption completed, the mixture was filtered and the biochar was collected. The biochar obtained was washed several times using DW and then dried. The above steps were repeated 5 times and the removal efficiency of Cd(II) by biochar was calculated.

2.5. Determination of released metal ions

The cations concentration (Na^+ and Ca^{2+}) in the solution after adsorption was determined using flame atomic absorption at different initial Cd(II) concentrations, while a blank group (DW without Cd +10 mg adsorbent) was set up for comparison. Then, the net release of cations was calculated.

2.6. Characterisation

The crystalline structure was analysed by X-ray diffraction (XRD, D8, Bruker, Germany). Surface morphological features and elemental content were analysed by scanning electron microscopy-energy-dispersive X-ray spectrometer (SEM-EDS, SUPRA 40, Zeiss, Germany). Fourier-transform infrared spectrometer (FTIR, 1725X, PerkinElmer, USA) was used to analyse functional groups of the adsorbents, with a scanning wavelength range of 400~4,000 cm^{-1} and a resolution of 0.3 cm^{-1}. The fully automated specific surface area and pore size analyser (ASAP 2020M, Micromeritics, USA) was used to analyse specific surface and pore size. The zeta potential analyser (Zetasizer Nano ZSE, Malvern, UK) analysed surface potential of biochar at different pH and calculated its zero potential point (pH_{ZPC}).

3. Results and discussion

3.1. Characterization analysis

As shown in Table 1, the specific surface area, pore volume and pore size of BC were 5.49 m^2/g, 0.054 cm^3/g and 9.57 nm, respectively. Nevertheless, the specific surface area, pore volume and pore size of MBBC were 201.24 m^2/g, 0.187 cm^3/g and 16.60 nm, respectively. This phenomenon demonstrated that ball milling could improve the pore structure of the biochar [22]. After Fe_3O_4-modified, the specific surface area, pore volume and pore size of Fe_3O_4@MBBC were 78.18 m^2/g, 0.108 cm^3/g and 13.69 nm, respectively. This can be attributed to the surface of MBBC was occupied by Fe_3O_4 particles, resulting in the reduction of pore structure [15]. The pH_{ZPC} of BC, MBBC and Fe_3O_4@MBBC were 4.67, 4.86 and 5.64, respectively. This indicated that when the pH solution was below pH_{PZC}, the adsorbent surface was positively charged and vice versa [16,26].

The microstructure and elemental composition were analysed by SEM-EDS. As shown in Fig. 1a, the surface of the BC was smooth and had a few pores. Furthermore, the main elements on the surface of the BC were C (30.21 wt.%), O (46.75 wt.%), Ca (6.32 wt.%) and Si (16.42 wt.%). After ball milling the pretreated raw material (Fig. 1b), the surface of the MBBC developed grooves and became rough. Notably, the MBBC shown an increase in the elemental content of O. Massive particulate matter appeared on the surface of the Fe_3O_4@MBBC (Fig. 1c). This may be responsible for the reduced pore structure of the Fe_3O_4@MBBC [25]. Notably, the element of Fe (12.39 wt.%) was present, which indicated that the Fe_3O_4 was successfully loaded on BC. Additionally, there was an increase in the content of element O.

The N_2 adsorption–desorption isotherm of the adsorbent is shown in Fig. 2a. As the relative pressure increased, the N_2 adsorption capacity by the biochars gradually increased and a hysteresis loop was formed. This confirmed that the adsorbent was a mesoporous material [4,23,26]. The pore-size distribution is shown in Fig. 2b. The pore-size distribution was concentrated between 2~50 nm, which indicated that the biochar was a mesoporous material [27,28]. Additionally, the pore sizes of BC, MBBC and Fe_3O_4@MBBC were 9.57, 16.60 and 13.75 nm, respectively.

As shown in Fig. 2c, in the FTIR spectrum BC had groups such as –OH (3,383 cm^{-1}), C=O (1,626 cm^{-1}), –COOH (1,428 cm^{-1}), C–O (1,036 cm^{-1}) and Si–O (473 cm^{-1}) [1,12,28–33]. After ball milling the pretreated, the vibrational peaks of –OH (3,427 cm^{-1}), C=O (1,626 cm^{-1}) and –COOH (1,432 cm^{-1}) groups in MBBC appear enhanced. This was also consistent with previous studies [34]. In the FTIR spectrum of Fe_3O_4@MBBC, the Fe–O group appeared at 560 cm^{-1} indicating successful modification [34,35]. Notably, the –OH group appeared enhanced and shifted after the modification, presumably because of the –OH introduced by the Fe_3O_4 modification [9,25,36]. Previous literature had shown that iron oxide modified biochar is effective in improving the removal of heavy metals [35,37]. The results showed that O-containing groups in the adsorbent can be increased by pre-treating it in a ball mill and loading it with Fe_3O_4.

The material compositions of adsorbent were analysed by XRD (Fig. 2d). The main substances was SiO_2 and $CaCO_3$ in BC and MBBC [2,28,38]. However, the diffraction peaks at 2θ = 30.2°, 35.5° and 43.2° in the Fe_3O_4@MBBC were considered to be Fe_3O_4, indicating the composite was successful prepared [36,37]. It was also confirmed that the particulate matter on the surface of the Fe_3O_4@MBBC was Fe_3O_4.

3.2. Batch adsorption experiments

3.2.1. Effect of initial pH on the Cd(II) removal

At 25°C, with a dosage of 10 mg, a Cd(II) concentration of 10 mg/L, and a reaction time of 480 min, the effect of initial pH (2.0~8.0) on Cd(II) removal was investigated. As shown in Fig. 3a, the Cd(II) removal efficiency by adsorbent increased rapidly followed by a slow increase. At pH = 6.0,

Table 1
Pore structure and zero potential point of adsorbent

	Specific surface area (m^2/g)	Pore volume (cm^3/g)	Average pore size (nm)	pH_{PZC}
BC	5.49	0.054	9.57	4.67
MBBC	201.24	0.187	16.60	4.86
Fe_3O_4@MBBC	78.18	0.108	13.75	5.64

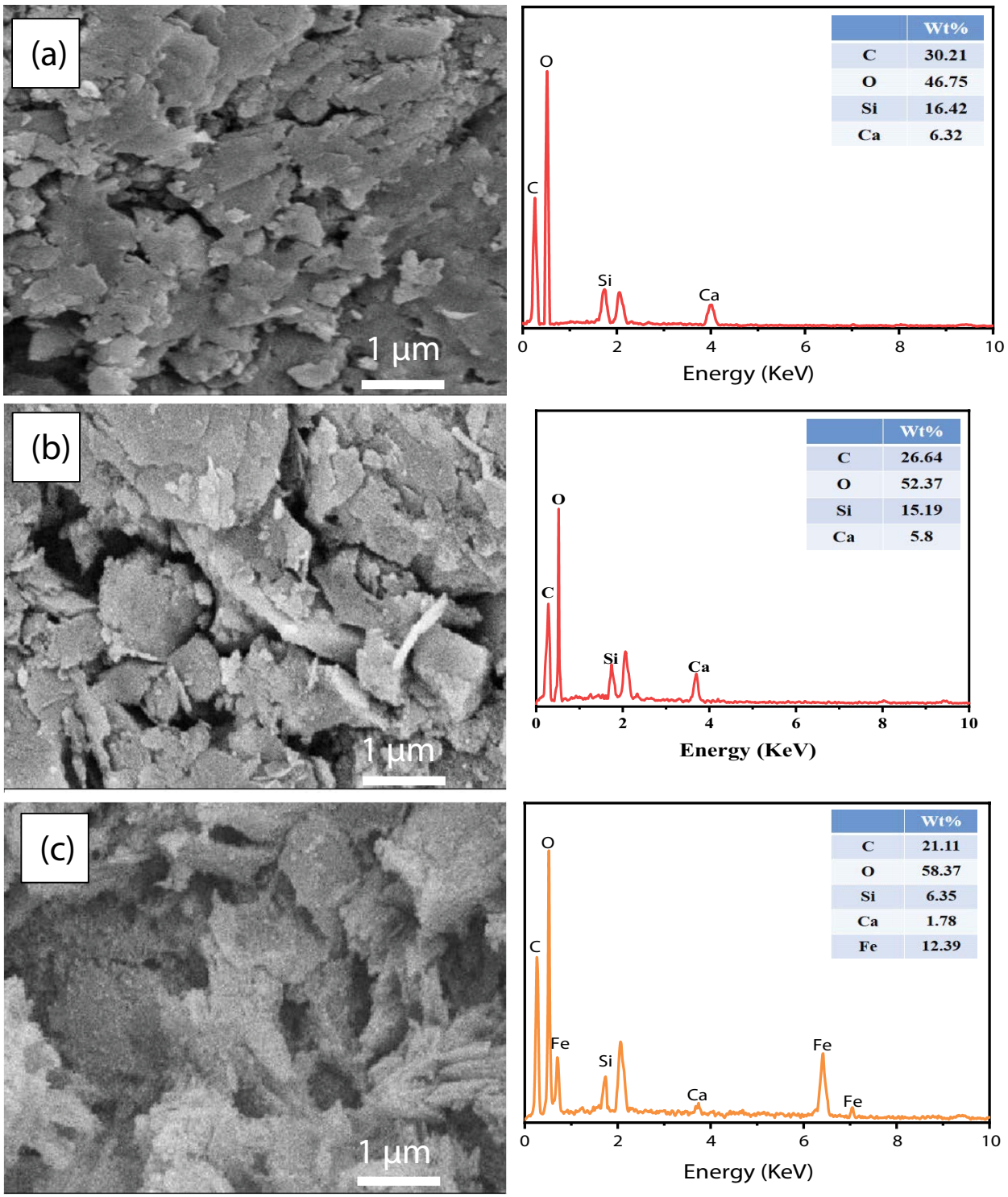

Fig. 1. SEM-EDS analysis of BC (a), MBBC (b) and Fe_3O_4@MBBC (c).

the removal efficiency of BC, MBBC and Fe_3O_4@MBBC were 67.37%, 78.72% and 96.77% respectively. At pH < 6.0, Cd(II) was mainly as Cd^{2+} in aqueous solution (Fig. S1a). When the pH of the solution exceeded 6.0, Cd(II) in solution appeared as $Cd(OH)_2$(s). The reason for this was presumed to be that at low pH, a large amount of H^+ occupied the biochar surface and protonated it, causing it to be positively charged [26,39]. The positively charged biochar on the surface created an electrostatic repulsion with the positively charged Cd(II), resulting in a low removal efficiency [25,31,40]. With increasing pH, the biochar deprotonated (biochar surface was negative charge) and thus enhanced

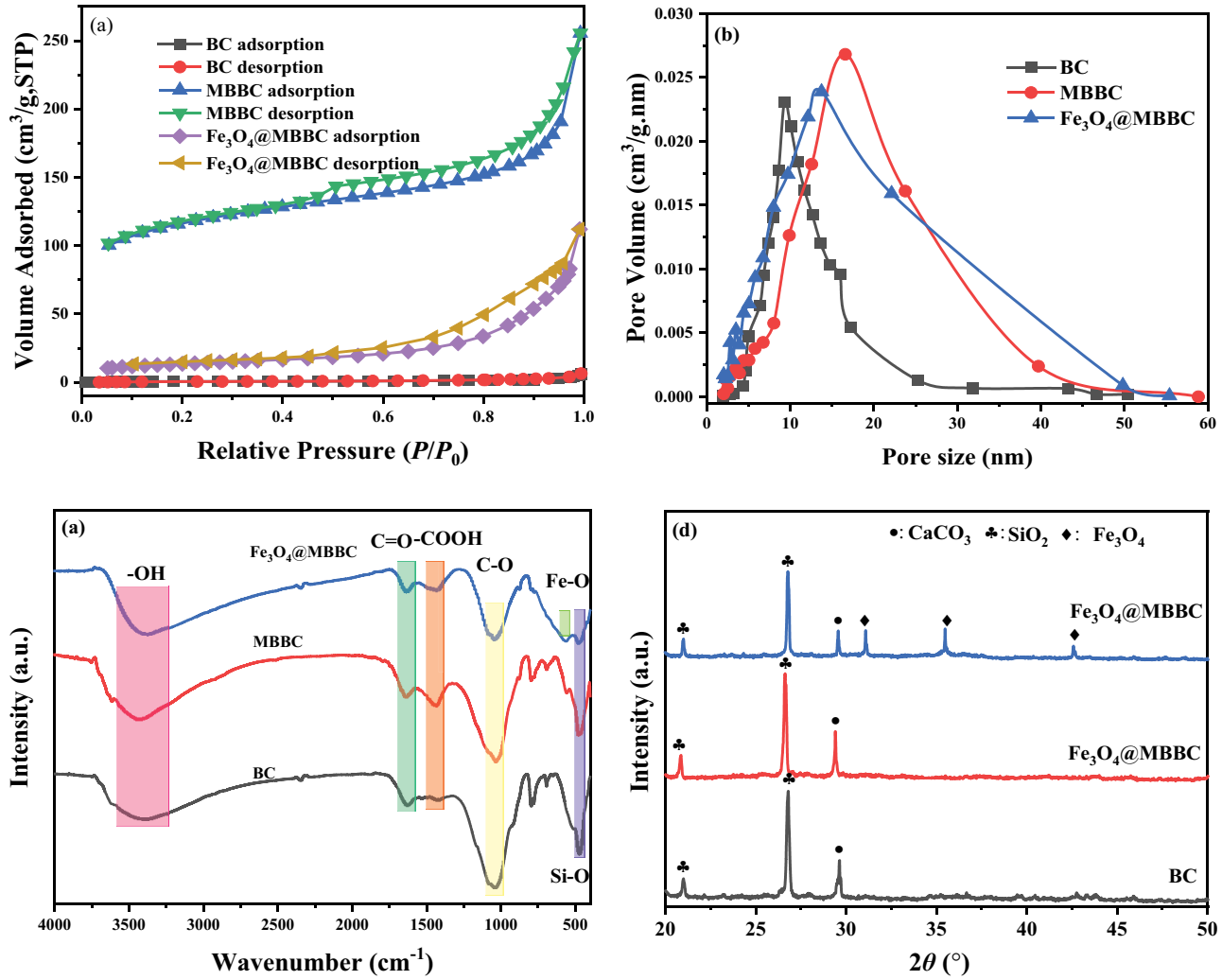

Fig. 2. N_2 adsorption–desorption isotherm (a), pore-size distribution (b), FTIR (c), and XRD (d) of adsorbent.

the Cd adsorption [25,41]. Notably, at pH > 6.0, the presence of $Cd(OH)_2$(s) precipitation also caused an increase in removal efficiency. To confirm the ability of biochar to promote the formation of Cd precipitates, the final pH after adsorption equilibrium was measured (Fig. S1b). The final pH of solutions was all higher than the initial pH, indicating that the adsorbent had a strong solution buffering capacity. Chen et al. [1] demonstrated that biochar had strong pH buffering capacity and was able to promote Cd precipitation from biochar. Additionally, previous literatures suggested that co-precipitation is one of the crucial mechanisms for the Cd removal from aqueous solutions by biochar [12,42].

Thus, electrostatic interaction and precipitation are involved in the removal of Cd(II).

3.2.1. Coexisting ions

The actual Cd(II)-containing wastewater is a more complex system, containing a variety of other cations (e.g., K^+, Na^+, Ni^{2+}, Pb^{2+}, Cu^{2+}, Fe^{3+} and Al^{3+}). The effect of coexisting ions (10~50 mg/L) on the Cd(II) removal is shown in Fig. 5c. The K^+ and Na^+ had almost no effect on the Cd(II) removal. However, the Ni^{2+}, Pb^{2+}, Cu^{2+}, Fe^{3+} and Al^{3+} caused a decrease in the adsorption efficiency. As the concentration of co-existing ions increased (from 0 to 50 mg/L), the removal of Cd(II) by the adsorbent decreased. Notably, the Pb^{2+} had a significant effect on the adsorption, followed by Cu^{2+} and Ni^{2+}. It was also possible that the affinity of the adsorbent for these 5 cations was higher than that of Cd(II), resulting in a significant inhibition of Cd(II) removal [43].

3.2.2. Background ions

The effect of the background ion (0~1 mol/L NaCl) on the Cd(II) removal was investigated at 10 mg dosage, 480 min reaction time, 10 mg/L Cd(II) concentration, initial pH 6.0 and 25°C. As shown in Fig. 5e, an increase in the ionic strength of NaCl from 0 mg/L to 1 mol/L had almost no effect on the Cd(II) removal. This result suggested that the Cd(II) removal on BC, MBBC and Fe_3O_4@MBBC was consistent with specific chemisorption [39]. This result

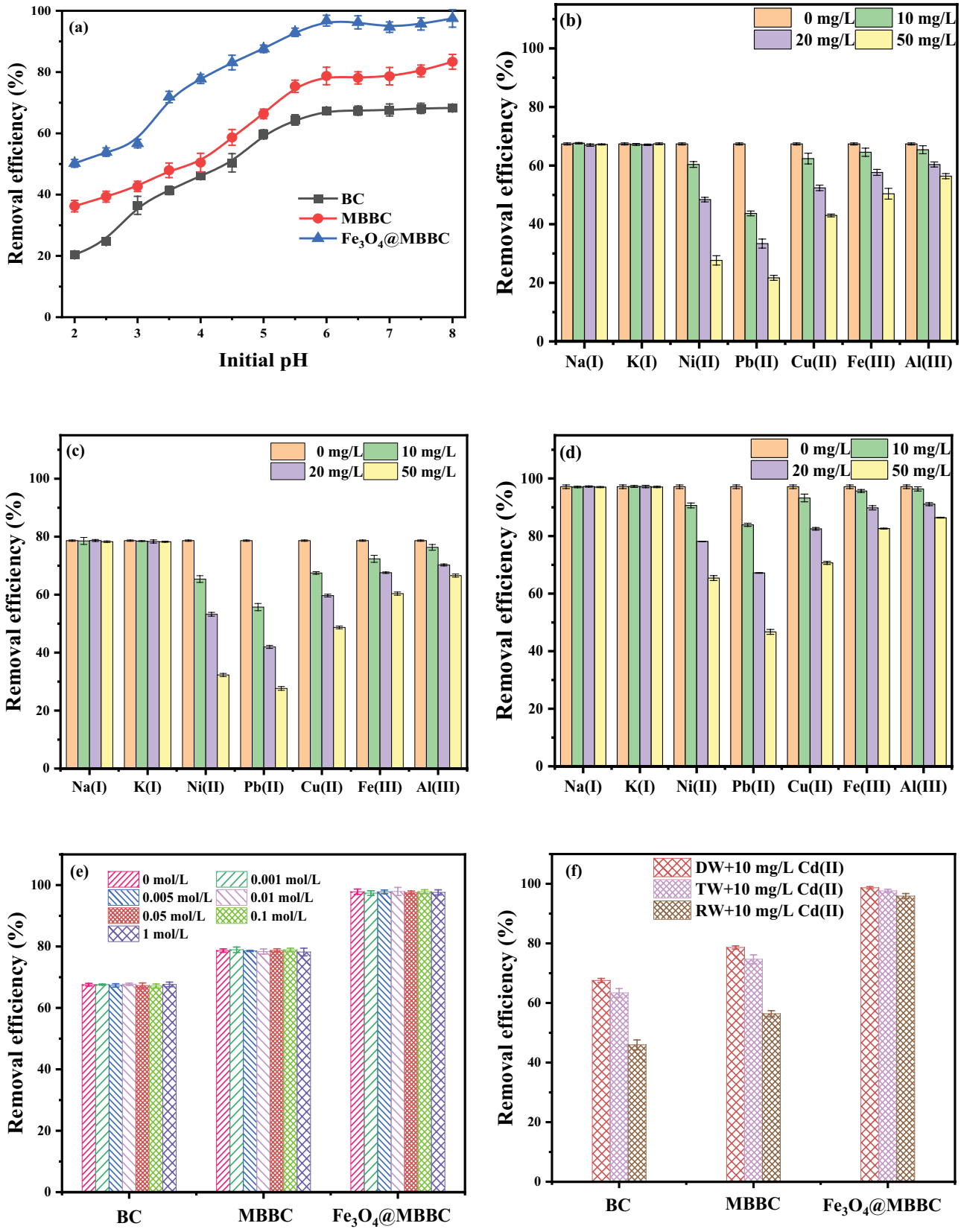

Fig. 3. Effect of the initial pH on the Cd(II) removal: (a) effect of coexisting ions on the Cd(II) removal by BC (b), MBBC (c) and Fe_3O_4@MBBC (d). The effect of background ion on Cd(II) removal (e). The effect of different water bodies on Cd(II) removal (f).

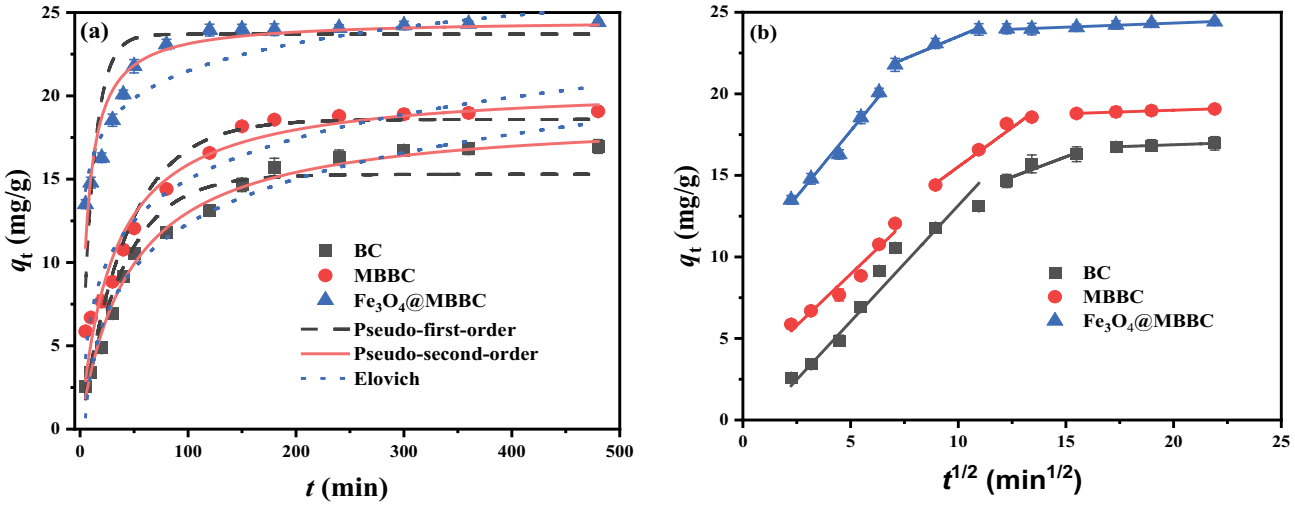

Fig. 4. Fitting of adsorption kinetics (a) and fitting of intraparticle diffusion model (b) for Cd(II).

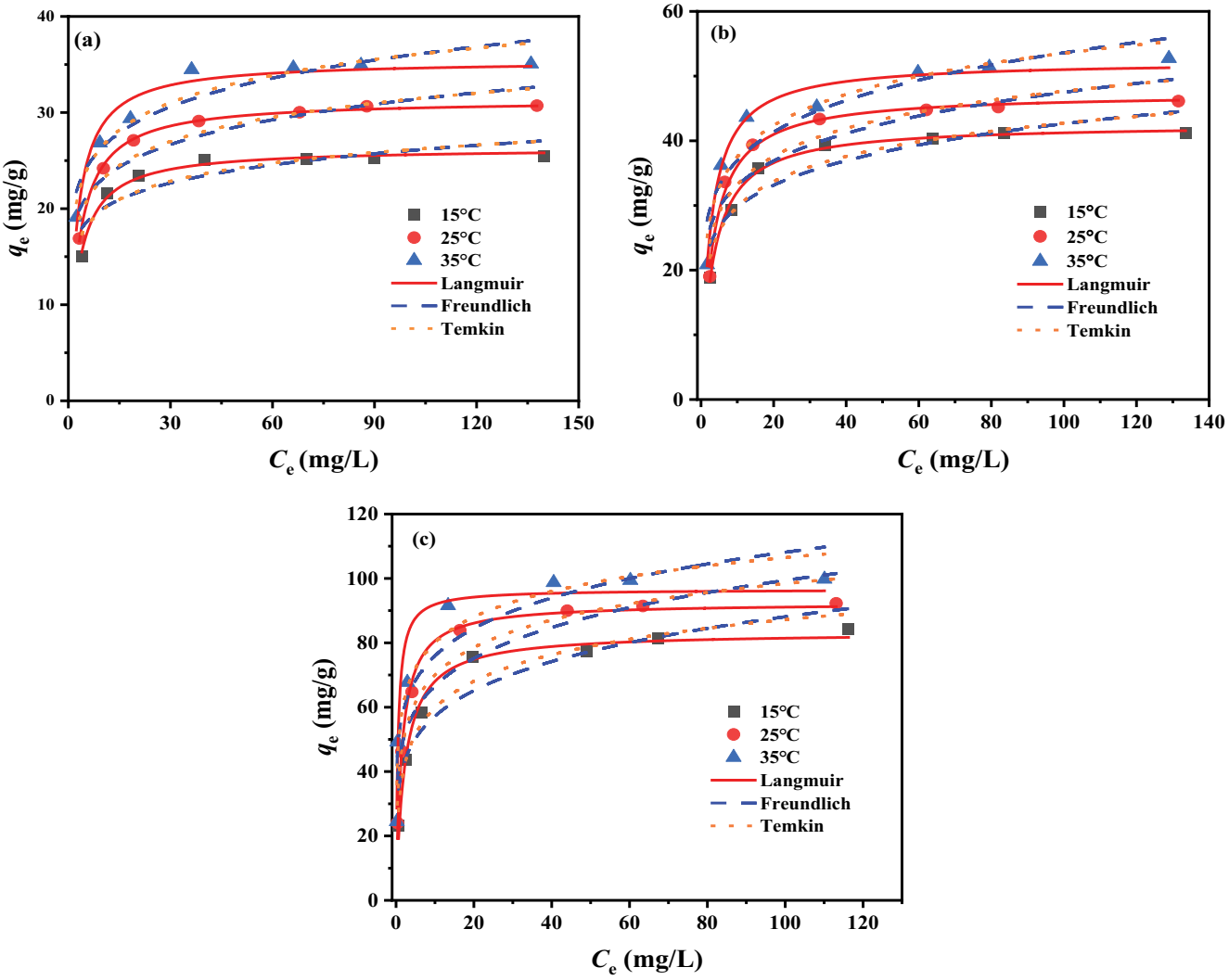

Fig. 5. Adsorption isotherm models for Cd(II) removal by BC (a), MBBC (b) and Fe_3O_4@MBBC (c).

indicated that the chemical reaction between Cd(II) and the adsorbent occurred (e.g., complexation with O-containing groups or co-precipitation) [43,44].

3.2.3. Removal of Cd(II) from actual water bodies

The removal of Cd(II) by biochar was tested in three different water bodies: deionized water (DW), tap water (TW), and river water (RW). As shown in Fig. 3f, the result showed that the Cd(II) removal efficiency of BC was 67.56% (DW), 63.39% (TW), and 45.94% (RW), respectively. The Cd(II) removal efficiency of MBBC was 78.64% (DW), 74.69% (TW), and 56.39% (RW), respectively. Notably, the Cd(II) removal efficiency in different water bodies by Fe_3O_4@MBBC was above 95%. The result confirmed that Fe_3O_4@MBBC was more effective in removing Cd(II) from the actual water bodies.

3.2.4. Adsorption kinetics

The effect of reaction time (5~480 min) was investigated at 25°C, dosage of 10 mg, Cd(II) concentration of 10 mg/L and pH 6.0 (Fig. 4). The adsorption capacity of BC, MBBC and Fe_3O_4@MBBC on Cd(II) increased rapidly to 13.10, 15.88 and 23.45 mg/g in 5~120 min, respectively. The adsorption capacity of BC, MBBC and Fe_3O_4@MBBC on Cd(II) increased slowly to 16.75, 18.89 and 24.23 mg/g in 120~300 min, respectively. The adsorption equilibrium was reached after 300 min. In the initial adsorption stage, the biochar surface had massive unused activity sites, resulting in a rapid increase in adsorption capacity [41,45]. With adsorption proceeded, available adsorption sites decreased, resulting in a slow increase in adsorption and finally reaching equilibrium [12,46]. Moreover, Fe_3O_4@MBBC had a higher adsorption capacity, presumably due to the Fe_3O_4-loaded providing more adsorption sites.

To further understand the Cd(II) removal process on biochar, the experimental data were fitted and analysed using pseudo-first-order model [Eq. (3)], pseudo-second-order model [Eq. (4)], Elovich model [Eq. (5)] and intraparticle diffusion model [Eq. (6)]. The results are shown in Fig. 4 and Table 2.

$$q_t = q_e\left(1 - e^{-k_1 t}\right) \tag{3}$$

$$q_t = \frac{q_e^2 k_2 t}{1 + q_e k_2 t} \tag{4}$$

$$q_t = \frac{1}{\beta}\ln\left(\alpha\beta t\right) \tag{5}$$

$$q_t = K_d t^{1/2} + C_i \tag{6}$$

where q_e and q_t are the adsorption capacity at adsorption equilibrium and at time "t", respectively, mg/g; k_1 (1/min) and k_2 (g/(mg·min)) are the pseudo-first-order model adsorption constant and pseudo-second-order model adsorption constant, respectively; α (mg/g·min) and β (g/mg) are the initial absorbance and desorption constant, respectively; K_d (mg/(m·min$^{1/2}$)) and C_i are intraparticle diffusion constant and boundary layer constant.

As shown in Table 2, the correlation coefficient of the pseudo-first-order model and the Elovich model was smaller than that of the pseudo-second-order model, indicating that the pseudo-second-order model could more accurately describe the process of Cd(II) adsorption by BC, MBBC and Fe_3O_4@MBBC [7,46,47]. Meanwhile, this result indicated that the Cd(II) removal on the two biochars was chemisorption [24,40,48]. As shown in Fig. 4b, the intraparticle diffusion model divided the adsorption process into 3 stages. The first stage was the diffusion of Cd(II) from the liquid membrane to the surface layer of the biochar; the second-stage was the diffusion of Cd(II) from the surface layer to the pore space; and the third stage was the adsorption equilibrium stage [31]. In addition, the intraparticle diffusion constants $K_{d1} > K_{d2} > K_{d3}$ and the boundary layer constants $C_1 < C_2 < C_3$ (Table 2) indicated that the first diffusion stage dominated the adsorption process [31,36].

3.2.5. Adsorption isotherms

The effect of the initial Cd(II) concentration (10~150 mg/L) and the adsorption temperature (15°C, 25°C and 35°C) on biochar was investigated at pH 6.0, dosage of 10 mg and a reaction time of 480 min. As shown in Fig. 5, the Cd(II) adsorption on BC, MBBC and Fe_3O_4@MBBC increased rapidly and then reached stability. Meanwhile, higher adsorption temperatures could promote the Cd(II) adsorption, which indicated that the Cd(II) adsorption on BC, MBBC and Fe_3O_4@MBBC was a heat absorption reaction. To further analyse the Cd(II) removal process, the experimental data were fitted and analysed by Langmuir model [Eq. (7)], Freundlich model [Eq. (8)] and Temkin model [Eq. (9)].

$$q_e = \frac{q_{\max} K_L C_e}{1 + K_L C_e},\ R_L = \frac{1}{1 + K_L C_0} \tag{7}$$

$$q_e = K_f C_e^{1/n} \tag{8}$$

$$q_e = \frac{RT}{b_T}\ln\left(A_T C_e\right) \tag{9}$$

is the Cd(II) concentration at adsorption equilibrium, mg/L; $q_{\max}$ (mg/g) and K_L (L/mg) are the theoretical maximum adsorption capacity and the Langmuir adsorption equilibrium constant, respectively; K_f (mg^{1-n} L^n/g) and n denoted the Freundlich adsorption equilibrium constant and the dimensionless number, respectively; A_T (1/g) and b_T (kJ/mol) are Temkin constants; R is gas constant (8.314 J/mol K), and T is the absolute temperature (K).

As shown in Table 3, the correlation coefficient of Langmuir model was the largest, which indicated that the Langmuir model better illustrated the Cd(II) removal process. This result also reflected the removal process as a homogeneous, monolayer adsorption [2,13,14,45]. Temperature increase was effective in increasing Cd(II) adsorption [16,29,38,46]. At 25°C, the maximum theoretical adsorption capacities of BC, MBBC and Fe_3O_4@MBBC were 31.33, 47.36 and 92.42 mg/g, respectively. At the same

Table 2
Kinetic model fitting parameters

	Pseudo-first-order			Pseudo-second-order			Elovich		
	q_e	k_1	R^2	q_e	k_2	R^2	α	β	R^2
BC	15.29	0.025	0.979	18.90	0.001	0.996	0.937	0.258	0.988
MBBC	18.59	0.023	0.906	20.70	0.002	0.950	2.38	0.280	0.943
Fe_3O_4@MBBC	23.70	0.090	0.700	24.57	0.007	0.923	190.70	0.418	0.909
	Intraparticle diffusion								
	K_{d1}	C_1	R^2	K_{d2}	C_2	R^2	K_{d3}	C_3	R^2
BC	0.082	1.424	0.989	8.714	0.495	0.932	15.954	0.046	0.999
MBBC	2.654	1.258	0.960	5.896	0.963	0.981	18.137	0.043	0.992
Fe_3O_4@MBBC	9.695	1.605	0.985	18.022	0.549	0.975	23.334	0.050	0.967

Table 3
Fitting parameters of adsorption isotherm model

		Langmuir			Freundlich			Temkin		
		q_{max}	K_b	R_1^2	K_f	n	R_2^2	b_T	A_T	R_2^2
BC	15°C	26.32	0.316	0.990	15.33	8.69	0.737	0.88×10^3	147.58	0.793
	25°C	31.33	0.349	0.998	16.98	7.53	0.841	0.68×10^3	57.81	0.896
	35°C	35.42	0.426	0.956	19.37	7.45	0.868	0.62×10^3	64.63	0.917
MBBC	15°C	42.57	0.306	0.994	20.71	6.38	0.819	0.42×10^3	20.21	0.889
	25°C	47.36	0.321	0.989	23.06	6.37	0.775	0.40×10^3	20.12	0.849
	35°C	52.30	0.392	0.983	25.51	6.20	0.853	0.37×10^3	22.58	0.916
Fe_3O_4@MBBC	15°C	83.26	0.446	0.985	37.13	5.33	0.881	0.20×10^3	15.39	0.955
	25°C	92.42	0.682	0.991	44.65	5.77	0.865	0.20×10^3	29.30	0.946
	35°C	96.59	1.963	0.927	53.33	6.52	0.860	0.22×10^3	109.11	0.923

temperature, Fe_3O_4@MBBC had a smaller partition coefficient R_L compared to BC and MBBC (Fig. S2), which indicated that Fe_3O_4@MBBC had a higher affinity for Cd(II) [31]. In addition, increasing the temperature also caused a decrease in R_L, suggesting that the increase in temperature favours adsorption [31,45]. The q_{max} values of Cd(II) for different types of adsorbent were listed in Table S1. The q_{max} of Cd(II) for different adsorbent varies greatly. In this work, the q_{max} of Fe_3O_4@MBBC was greater than that of the adsorbent, indicating that Fe_3O_4@MBBC had great potential to become a powerful adsorbent.

3.3. Mechanism analysis of Cd(II) removal

FTIR (Fig. 6a) was used to analyse the changes of functional groups before and after the Cd(II) adsorption. The OH group's vibrational peak shifted and weakened. Moreover, the peaks of C=O, –COOH and C–O groups became weakened. The Fe–O group was also weakened after adsorption. This phenomenon indicated that the –OH, C=O, –COOH, C–O and Fe–O groups were involved in the adsorption of Cd(II) [1,13,17,25]. Previous research has shown that O-containing groups in biochar can complex with Cd(II) [12,42]. Furthermore, the literature confirmed that the weakening of Fe–O was caused by complexation with heavy metals [18,25,37]. The weakening of the O-containing groups (C–O, –OH, –COOH and C=O) was considered to be a complexation reaction with heavy metals [12,16,17,26]. The analysis showed that the mechanism of Cd(II) removal included complexation with O-containing function groups.

The crystal structure before and after the Cd(II) adsorption was analysed using XRD (Fig. 6b). After adsorption, the diffraction peaks of both Fe_3O_4 and $CaCO_3$ appeared to be weakened. Notably, $Cd(OH)_2$ and $CdCO_3$ precipitates appeared at $2\theta = 22.56°$ and 36.39°, respectively [49]. The presence of $Cd(OH)_2$ suggested that Cd(II) precipitated during the adsorption process, which was also consistent with previous studies [42,49]. Furthermore, previous research has shown that carbonates in biochar are released into solution and combine with Cd(II), resulting in $CdCO_3$ precipitates [1,6,49]. Therefore, the mechanism of Cd(II) removal included co-precipitation.

To further confirm the adsorption mechanism (Fig. S3), whether ion exchange occurred was confirmed by measuring the net release of Na^+ and Ca^{2+} from the solution. The Cd(II) adsorption capacity correlated positively with the net release of cations. This finding implies that the cations exchanged with Cd(II), removing Cd(II) from the solution [6,49,50]. The highest Ca^{2+} concentration was released, which also indicated that Ca^{2+} played a major role in the ion

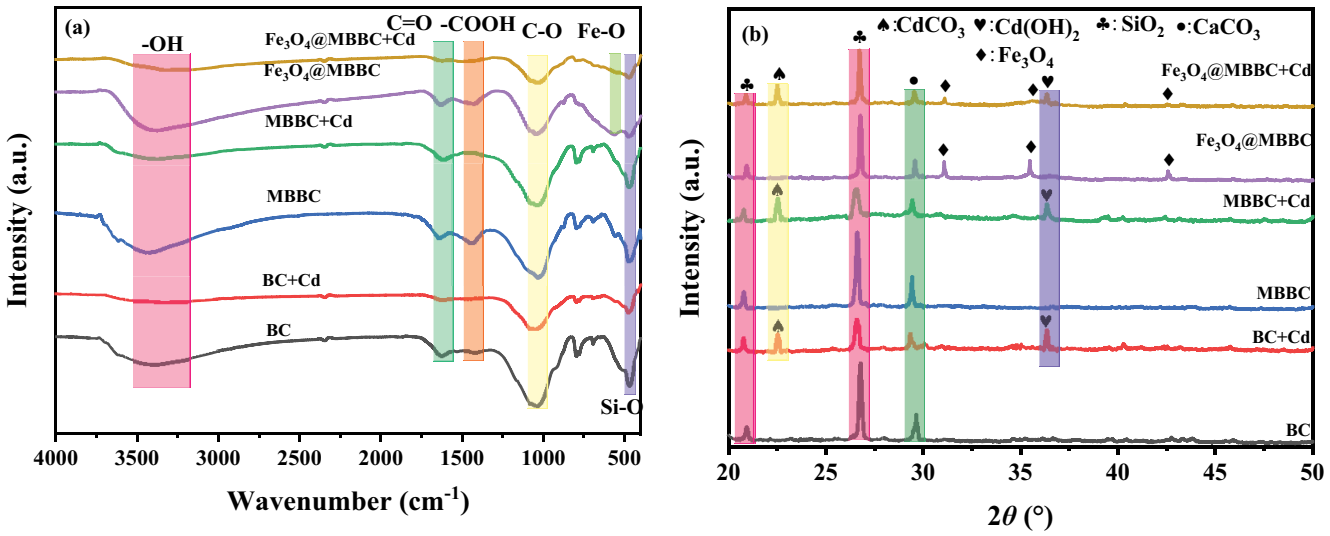

Fig. 6. FTIR (a) and XRD (b) analysis before and after Cd(II) adsorption.

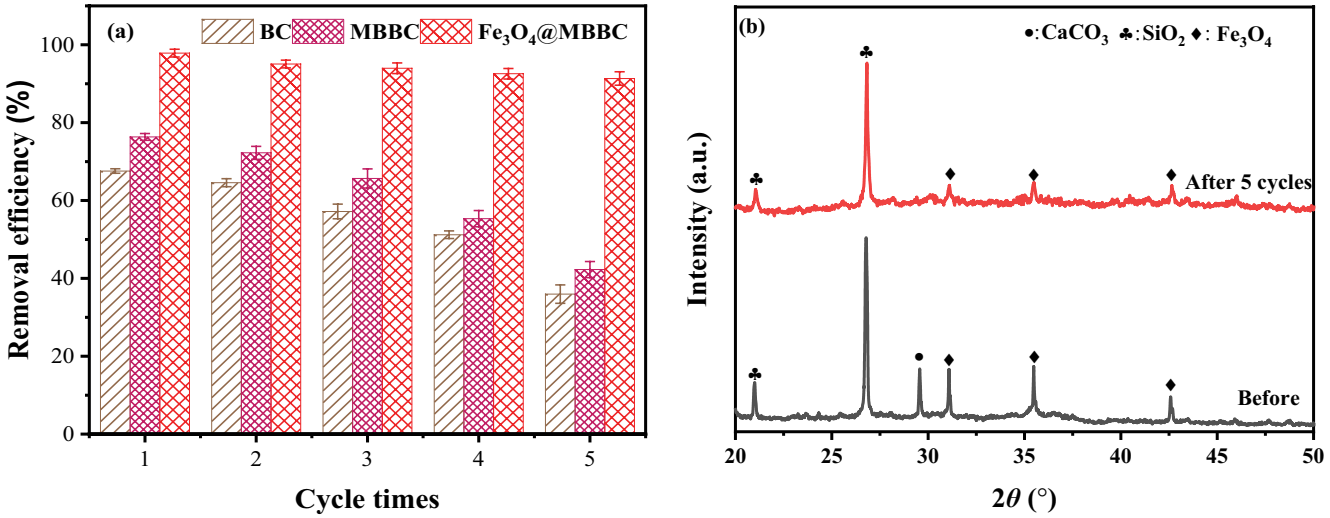

Fig. 7. Adsorption–desorption experiments of BC, MBBC and Fe_3O_4@MBBC (a). XRD analysis of Fe_3O_4@MBBC after 5 adsorption–desorption experiments (b).

exchange process. This result was also consistent with previous studies [42,50]. Also, the amount of cations released by BC and MBBC was higher than that of Fe_3O_4@MBBC, which suggests that the Fe_3O_4 loading would lower the adsorbent's ability to exchange ions.

Therefore, the removal mechanism included complexation, ion exchange, co-precipitation and electrostatic interaction.

3.4. Adsorption–desorption experiments

Fig. 7 depicts the results of five adsorption–desorption experiments performed at pH 6.0, a dosage of 10 mg, a Cd(II) concentration of 10 mg/L, an adsorption time of 480 min, and a temperature of 25°C. The results showed that the removal efficiency of BC decreased from about 76.35% to 52.27%, while the removal efficiency of Fe_3O_4@MBBC remained above 91.35%. This suggested that Fe_3O_4@MBBC could be used to improve removal efficiency and the removal of Cd(II)-contaminated wastewater. Besides, to confirm the stability of the adsorbent, XRD analysis of Fe_3O_4@MBBC after five adsorption–desorption experiments is shown in Fig. 7b. After five adsorption–desorption experiments, the diffraction peaks of $CaCO_3$ disappeared, and the diffraction peaks of SiO_2 and Fe_3O_4 appeared to be weakened. The crystalline structure of Fe_3O_4@MBBC remained essentially unchanged after five adsorption–desorption experiments, indicating that the stability of Fe_3O_4@MBBC was still good.

4. Conclusion

The results demonstrated that ball mill pretreatment and Fe_3O_4 loading can effectively increase the content of O-containing groups in the adsorbent. The pseudo-second-order kinetic model and the Langmuir isotherm model were used to explain the adsorption processes of BC, MBBC,

and Fe_3O_4@MBBC on Cd(II). In addition, the maximum adsorption capacities of BC, MBBC and Fe_3O_4@MBBC were 31.33, 47.36 and 92.42 mg/g, respectively. The mechanisms of Cd(II) removal were complexation, ion exchange, co-precipitation and electrostatic interaction. The removal efficiency of Cd(II) on Fe_3O_4@MBBC remained above 91.35% after five adsorption–desorption experiments, indicating that Fe_3O_4@MBBC had the potential to be better applied for Cd(II) removal from aqueous solutions.

Funding

This work was supported by National Natural Science Foundation of China (5167081086).

Conflicts of interest

The author declare that I have no competing financial interests.

References

[1] T. Chen, Z.Y. Zhou, H. Rong, R.H. Meng, H.T. Wang, W.J. Lu, Adsorption of cadmium by biochar derived from municipal sewage sludge: impact factors and adsorption mechanism, Chemosphere, 134 (2015) 286–293.
[2] L. Dai, J. Ren, L. Tao, C. Chen, Properties of sewage sludge biochar produced under different pyrolysis temperatures and its sorption capability to Cd^{2+}, Chin. J. Environ. Eng., 11 (2017) 4029–4035.
[3] J.Y. Zhang, M.W. Yan, G.C. Sun, K.Q. Liu, Simultaneous removal of Cu(II), Cd(II), Cr(VI), and rhodamine B in wastewater using TiO_2 nanofibers membrane loaded on porous fly ash ceramic support, Sep. Purif. Technol., 272 (2021) 118888, doi: 10.1016/j.seppur.2021.118888.
[4] J. Chen, R. Huang, H. Ouyang, G.W. Yu, Y.H. Liang, Q. Zheng, Utilization of dredged river sediments to synthesize zeolite for Cd(II) removal from wastewater, J. Cleaner Prod., 320 (2021) 128861, doi: 10.1016/j.jclepro.2021.128861.
[5] L.Y. Gao, J.H. Deng, G.Q. Tang, X.N. Huang, Z.K. Cai, Y.X. Cai, F. Huang, Adsorption characteristics and mechanism of Cd^{2+} on biochar with different pyrolysis temperatures produced from eucalyptus leaves, China Environ. Sci., 38 (2018) 1001–1009.
[6] W.Q. Zuo, C. Chen, H.J. Cui, M.L. Fu, Enhanced removal of Cd(II) from aqueous solution using $CaCO_3$ nanoparticle modified sewage sludge biochar, RSC Adv., 7 (2017) 16238–16243.
[7] S.H. Zhu, Q. Ting, M.K. Irshad, J.Y. Shang, Simultaneous removal of Cd(II) and As(III) from co-contaminated aqueous solution by α-FeOOH modified biochar, Biochar, 2 (2020) 81–92.
[8] J.J. Wang, R. Chen, L. Fan, L.L. Cui, Y.J. Zhang, J.J. Cheng, X.L. Wu, W.M. Zeng, Q.H. Tian, L. Shen, Construction of fungi-microalgae symbiotic system and adsorption study of heavy metal ions, Sep. Purif. Technol., 268 (2021) 118689, doi: 10.1016/j.seppur.2021.118689.
[9] R.F. Wang, Y.N. Zhou, H.B. Meng, H.Z. Yang, Adsorption of Cd in solution by different modified biochar, J. Agric. Sci. Technol., 18 (2016) 103–111.
[10] Z.Y. Wang, G.C. Liu, F.M. Li, H. Zheng, Adsorption of Cd(II) varies with biochars derived at different pyrolysis temperatures, Environ. Sci., 35 (2014) 4735–4744.
[11] K.Q. Zheng, J.C. Wang, S.T. Liu, H.B. Xue, J.Y. Wu, T.Y. Liu, W.Q. Yin, X.Z. Wang, Adsorption characteristic of Pb^{2+} and Cd^{2+} with sludge biochars derived atdifferent pyrolysis temperatures, Chin. J. Environ. Eng., 10 (2016) 7277–7282.
[12] S. Cheng, Y.Z. Liu, B.L. Xing, X.J. Qin, G.X. Zhang, H.Y. Xia, Lead and cadmium clean removal from wastewater by sustainable biochar derived from poplar saw dust, J. Cleaner Prod., 314 (2021) 128074, doi: 10.1016/j.jclepro.2021.128074.
[13] W.H. Du, W.Q. Zhu, X.H. Pan, X.Y. Shen, S.Y. Chen, K.L. Chen, K. Mushala, H.J. Zhang, Y. Ding, Adsorption of Pb^{2+} and Cd^{2+} from aqueous solution using vermicompost derived from cow manure and its biochar, Environ. Sci., 38 (2017) 2172–2181.
[14] J. Liang, X.M. Li, Z.G. Yu, G.M. Zeng, Y. Luo, L.B. Jiang, Z.X. Yang, Y.Y. Qian, H.P. Wu, Amorphous MnO_2 modified biochar derived from aerobically composted swine manure for adsorption of Pb(II) and Cd(II), ACS Sustainable Chem. Eng., 5 (2017) 5049–5058.
[15] H. Liang, Z.H. Luo, H.Y. Zhao, Y.T. Feng, Y.H. Liang, M. Xu, The adsorption of Cd^{2+} in the aqueous solution by 7 modified rice straws, China Environ. Sci., 38 (2018) 596–607.
[16] S.H. Cui, R. Zhang, Y.T. Peng, G. Xing, Z. Li, B.B. Fan, C.Y. Guan, J.Z. Beiyuan, Y.Y. Zhou, J. Liu, Q. Chen, J. Sheng, L.L. Guo, New insights into ball milling effects on MgAl-LDHs exfoliation on biochar support: a case study for cadmium adsorption, J. Hazard. Mater., 416 (2021) 126258, doi: 10.1016/j.jhazmat.2021.126258.
[17] R.Q. Chen, X. Zhao, J. Jiao, Y. Li, M. Wei, Surface-modified biochar with polydentate binding sites for the removal of cadmium, Int. J. Mol. Sci., 20 (2019) 1775–1790.
[18] L.L. Ling, W.J. Liu, S. Zhang, H. Jiang, Magnesium oxide embedded nitrogen self-doped biochar composites: fast and high-efficiency adsorption of heavy metals in an aqueous solution, Environ. Sci. Technol., 51 (2017) 10081–10089.
[19] Y.P. Zhang, Z.Y. Chen, C.H. Chen, F.Z. Li, K. Shen, Effects of UV-modified biochar derived from phytoremediation residue on Cd bioavailability and uptake in *Coriandrum sativum* L. in a Cd-contaminated soil, Environ. Sci. Pollut. Res., 28 (2021) 17395–17404.
[20] G. Cao, J.X. Sun, M.H. Chen, H.M. Sun, G.L. Zhang, Co-transport of ball-milled biochar and Cd^{2+} in saturated porous media, J. Hazard. Mater., 416 (2021) 125725, doi: 10.1016/j.jhazmat.2021.125725.
[21] B. Wang, D. Ai, Y. Meng, D.Q. Wei, Y.N. Tang, R. Yang, Application advances of ball milling modified biochar in environmental remediation, Fine Chem., 39 (2022) 217–301.
[22] S.O. Amusat, T.G. Kebede, S. Dube, M.M. Nindi, Ball-milling synthesis of biochar and biochar-based nanocomposites and prospects for removal of emerging contaminants: a review, J. Water Process Eng., 41 (2021) 101993, doi: 10.1016/j.jwpe.2021.101993.
[23] J. Xiao, R. Hu, G.C. Chen, Micro-nano-engineered nitrogenous bone biochar developed with a ball-milling technique for high-efficiency removal of aquatic Cd(II), Cu(II) and Pb(II), J. Hazard. Mater., 387 (2019) 121980, doi: 10.1016/j.jhazmat.2019.121980.
[24] B. Wang, B. Gao, Y.S. Wan, Entrapment of ball-milled biochar in Ca-alginate beads for the removal of aqueous Cd(II), J. Ind. Eng. Chem., 61 (2018) 161–168.
[25] T. Chen, Z.Y. Zhou, R.H. Meng, Y.T. Liu, H.T. Wang, W.J. Lu, J. Jin, Y. Liu, Characteristics and heavy metal adsorption performance of sewage sludge-derived biochar from co-pyrolysis with transition metals, Environ. Sci., 40 (2019) 324–330.
[26] H.H. Lyu, B. Gao, F. He, A.R. Zimmerman, C. Ding, H. Huang, J.C. Tang, Effects of ball milling on the physicochemical and sorptive properties of biochar: experimental observations and governing mechanisms, Environ. Pollut., 233 (2018) 54–63.
[27] F.J. Lopez-Tenllado, I.L. Motta, J.M. Hill, Modification of biochar with high-energy ball milling: development of porosity and surface acid functional groups, Bioresour. Technol. Rep., 15 (2021) 100704, doi: 10.1016/j.biteb.2021.100704.
[28] Y.H. Xing, X.S. Luo, S. Liu, W.J. Wan, Q.Y. Huang, W.L. Chen, A novel eco-friendly recycling of food waste for preparing biofilm-attached biochar to remove Cd^{2+} and Pb^{2+} in wastewater, J. Cleaner Prod., 311 (2021) 127514, doi: 10.1016/j.jclepro.2021.127514.
[29] S. Bashir, J. Zhu, Q.L. Fu, H.Q. Hu, Comparing the adsorption mechanism of Cd by rice straw pristine and KOH-modified biochar, Environ. Sci. Pollut. Res., 25 (2018) 11875–11883.
[30] X. Deng, H. Zhou, X.N. Qu, J. Long, P.Q. Peng, H.B. Hou, K.L. Li, P. Zhang, B.H. Liao, Optimization of Cd(II) removal from aqueous solution with modified corn straw biochar using

Plackett–Burman design and response surface methodology, Desal. Water Treat., 70 (2017) 210–219.
[31] F.F. Ma, B.W. Zhao, J.R. Diao, Adsorptive characteristics of cadmium onto biochar produced from pyrolysis of wheat straw in aqueous solution, China Environ. Sci., 37 (2017) 551–559.
[32] Z.D. Wu, X.M. Wang, J. Yao, S.Y. Zhan, H. Li, J. Zhang, Z.M. Qiu, Synthesis of polyethyleneimine modified $CoFe_2O_4$-loaded porous biochar for selective adsorption properties towards dyes and exploration of interaction mechanisms, Sep. Purif. Technol., 277 (2021) 119474, doi: 10.1016/j.seppur.2021.119474.
[33] J. Zhang, W.J. Lu, S.Y. Zhan, J.M. Qiu, X.M. Wang, Z.D. Wu, H. Li, Z.M. Qiu, H.L. Peng, Adsorption and mechanistic study for humic acid removal by magnetic biochar derived from forestry wastes functionalized with Mg/Al-LDH, Sep. Purif. Technol., 276 (2021) 119296, doi: 10.1016/j.seppur.2021.119296.
[34] Y. Li, J. Wen, Z.Z. Xue, Y.F. Li, C.L. Yang, X.Y. Yin, Microscopic investigation into remediation of cadmium and arsenite Co-contamination in aqueous solution by Fe-Mn-incorporated titanosilicate, Sep. Purif. Technol., 279 (2021) 119809, doi: 10.1016/j.seppur.2021.119809.
[35] M. Parastar, S. Sheshmani, S. Shokrollahzadeh, Cross-linked chitosan into graphene oxide-iron(III) oxide hydroxide as nano-biosorbent for Pd(II) and Cd(II) removal, Int. J. Biol. Macromol., 166 (2021) 229–237.
[36] F.F. Ma, B.W. Zhao, J.R. Diao, Adsorptive characteristics of cadmium onto biochar produced from pyrolysis of wheat straw in aqueous solution, China Environ. Sci., 39 (2019) 172–180.
[37] X.Y. Hu, Y.J. Chen, S.S. Zhang, X.Q. Wang, C.C. Li, X. Guo, Cd removal from aqueous solution using magnetic biochar derived from maize straw and its recycle, Trans. Chin. Soc. Agric. Eng., 34 (2018) 208–218.
[38] R. Ma, X.Q. Yan, X.C. Pu, X.Y. Fu, L.Q. Bai, Y.F. Du, M.X. Cheng, J. Qian, An exploratory study on the aqueous Cr(VI) removal by the sulfate reducing sludge-based biochar, Sep. Purif. Technol., 276 (2021) 119314, doi: 10.1016/j.seppur.2021.119314.
[39] J.Z. Zhang, X.F. Ma, L. Yuan, D.X. Zhou, Comparison of adsorption behavior studies of Cd^{2+} (by vermicompost biochar and $KMnO_4$-modified vermicompost biochar, J. Environ. Manage., 256 (2020) 109959, doi: 10.1016/j.jenvman.2019.109959.
[40] Y.H. Tan, X.R. Wan, X. Ni, L. Wang, T. Zhou, H.M. Sun, N. Wang, X.Q. Yin, Efficient removal of Cd(II) from aqueous solution by chitosan modified kiwi branch biochar, Chemosphere, 289 (2021) 133251, doi: 10.1016/j.chemosphere.2021.133251.
[41] Z.Y. Shao, J.L. Lu, J. Ding, F.J. Fan, X.Y. Sun, P. Li, Y. Fang, Q.H. Hu, Novel green chitosan-pectin gel beads for the removal of Cu(II), Cd(II), Hg(II) and Pb(II) from aqueous solution, Int. J. Biol. Macromol., 173 (2021) 217–225.
[42] J.W. Wu, T. Wang, J.W. Wang, Y.S. Zhang, W.-P. Pan, A novel modified method for the efficient removal of Pb and Cd from wastewater by biochar: enhanced the ion exchange and precipitation capacity, Sci. Total Environ., 754 (2021) 142150, doi: 10.1016/j.scitotenv.2020.142150.
[43] J. Deng, Y. Liu, S. Liu, G. Zeng, Z. Yan, Competitive adsorption of Pb(II), Cd(II) and Cu(II) onto chitosan-pyromellitic dianhydride modified biochar, J. Colloid Interface Sci., 506 (2017) 355–364.
[44] T.T. Yang, Y.M. Xu, Q.Q. Huang, Y.B. Sun, X.F. Liang, L. Wang, X. Qin, L.J. Zhao, Adsorption characteristics and the removal mechanism of two novel Fe-Zn composite modified biochar for Cd(II) in water, Bioresour. Technol., 333 (2021) 125078, doi: 10.1016/j.biortech.2021.125078.
[45] H. Chakhtouna, H. Benzeid, N. Zari, A.E.K. Qaiss, R. Bouhfid, Functional $CoFe_2O_4$-modified biochar derived from banana pseudostem as an efficient adsorbent for the removal of amoxicillin from water, Sep. Purif. Technol., 266 (2021) 118592, doi: 10.1016/j.seppur.2021.118592.
[46] L. Brinza, K. Geraki, A. Matamoros-Veloza, M. Ignat, M. Neamtu, The Irish kelp, *Fucus vesiculosus*, a highly potential green bio sorbent for Cd(II) removal: mechanism, quantitative and qualitative approaches, J. Cleaner Prod., 327 (2021) 129422, doi: 10.1016/j.jclepro.2021.129422.
[47] J.H. Cao, Q.L. Liu, Y.J. Huang, S.J. Tao, W.H. Qin, H.B. Ren, Effects of feedstock type and pyrolysis temperature on Cd^{2+} adsorption by biochar, Chem. Ind. Eng. Prog., 38 (2019) 4183–4190.
[48] C.F. Peng, T.X. Xiao, Z.J. Li, Effects of pyrolysis temperature on structural properties of sludge-based biochar and its adsorption for heavy metals, Res. Environ. Sci., 30 (2017) 1637–1644.
[49] J.W. Wu, T. Wang, Y.S. Zhang, W.P. Pan, The distribution of Pb(II)/Cd(II) adsorption mechanisms on biochars from aqueous solution: considering the increased oxygen functional groups by HCl treatment, Bioresour. Technol., 291 (2019) 121859, doi: 10.1016/j.biortech.2019.121859.
[50] N.N. Rong, C.C. Chen, K.W. Ouyang, K.J. Zhang, X.R. Wang, Z.Y. Xu, Adsorption characteristics of directional cellulose nanofiber/chitosan/montmorillonite aerogel as adsorbent for wastewater treatment, Sep. Purif. Technol., 274 (2021) 119120, doi: 10.1016/j.seppur.2021.119120.

Supplementary information

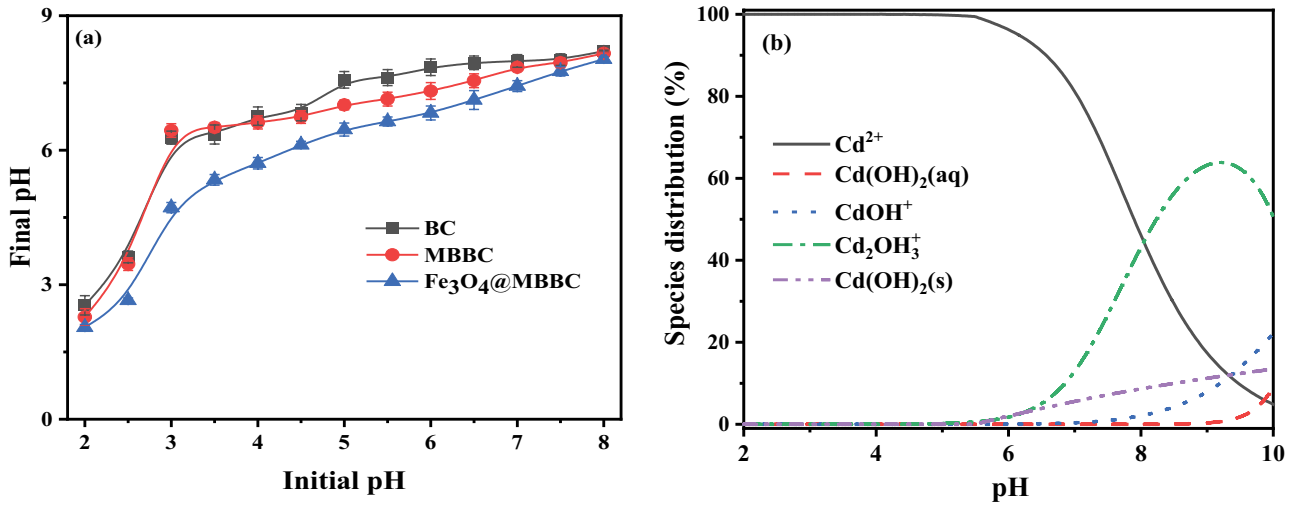

Fig. S1. The pH changes after adsorption equilibration (a). The distribution of Cd(II) species in aqueous solution at different pH (b).

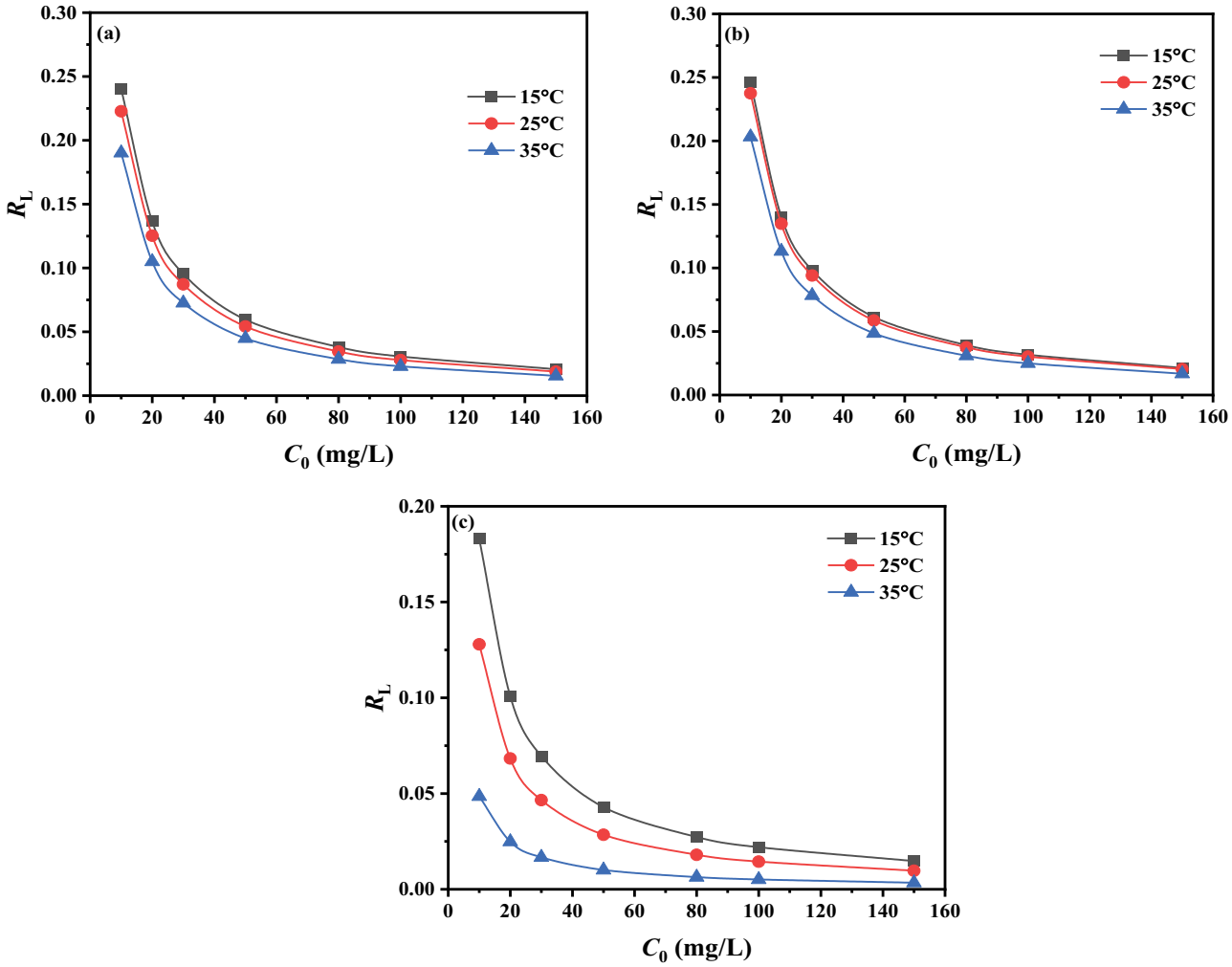

Fig. S2. Relationship between initial Cd(II) concentration and Langmuir model partition coefficient R_L (a) BC, (b) MBBC, and (c) Fe_3O_4@MBBC.

Table S1
Comparison of the Cd(II) adsorption capacity of Fe_3O_4@MBBC and other adsorbents

Adsorbent	Adsorption pH	q_{max} (mg/g)	References
α-FeOOH@BC	4.0	39.30	[S1]
Poplar saw dust-derived biochar	5.0	49.32	[S2]
KOH-modified rice straw biochar	6.5	41.90	[S3]
Cystamine dihydrochloride-modified rice husk biochar	7.0	81.02	[S4]
Fe/Zn-modified durian shells biochar	5.0	98.58	[S5]
BC	6.0	31.33	This work
MBBC	6.0	47.36	This work
Fe_3O_4@MBBC	6.0	92.43	This work

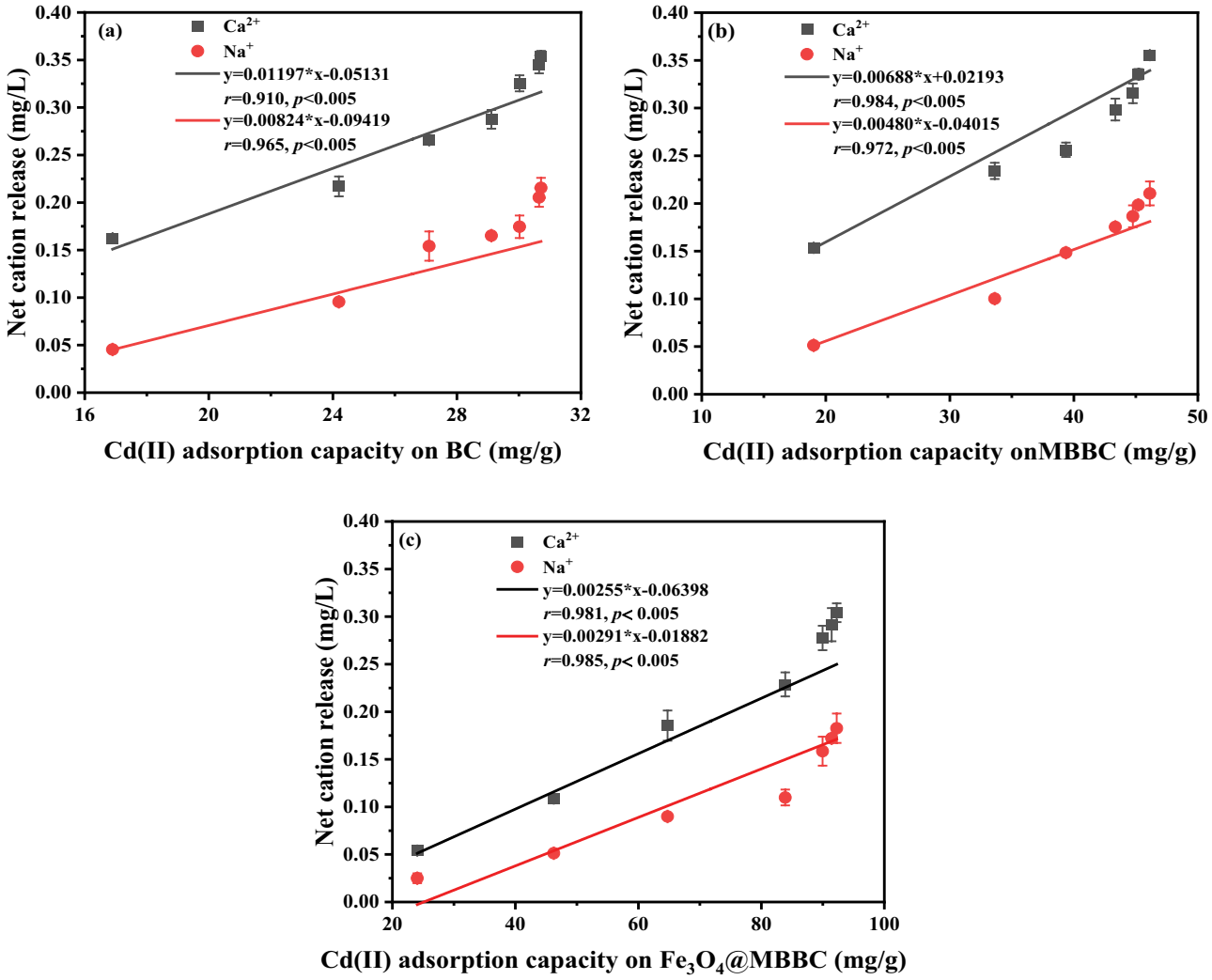

Fig. S3. Correlation analysis of Cd(II) adsorption capacity by BC (a), MBBC (b) and Fe_3O_4@MBBC (c) with net cation release.

References

[1] S.H. Zhu, Q. Ting, M.K. Irshad, J.Y. Shang, Simultaneous removal of Cd(II) and As(III) from co-contaminated aqueous solution by α-FeOOH modified biochar, Biochar, 2 (2020) 81–92.

[2] S. Cheng, Y.Z. Liu, B.L. Xing, X.J. Qin, G.X. Zhang, H.Y. Xia, Lead and cadmium clean removal from wastewater by sustainable biochar derived from poplar saw dust, J. Cleaner Prod., 314 (2021) 128074, doi: 10.1016/j.jclepro.2021.128074.

[3] S. Bashir, J. Zhu, Q.L. Fu, H.Q. Hu, Comparing the adsorption mechanism of Cd by rice straw pristine and KOH-modified biochar, Environ. Sci. Pollut. Res., 25 (2018) 11875–11883.

[4] R.Q. Chen, X. Zhao, J. Jiao, Y. Li, M. Wei, Surface-modified biochar with polydentate binding sites for the removal of cadmium, Int. J. Mol. Sci., 20 (2019) 1775–1790.

[5] T.T. Yang, Y.M. Xu, Q.Q. Huang, Y.B. Sun, X.F. Liang, L. Wang, X. Qin, L.J. Zhao, Adsorption characteristics and the removal mechanism of two novel Fe-Zn composite modified biochar for Cd(II) in water, Bioresour. Technol., 333 (2021) 125078, doi: 10.1016/j.biortech.2021.125078.